THESIS PRESENTED FOR THE DEGREE OF MASTER OF SCIENCE

Charge distribution in Neutron Stars

SAKHILE MPILO NDEBELE

School of Mathematics, Statistics and Computer Science College of Agriculture,

Engineering and Science

University of KwaZulu-Natal

Durban

Westville Campus, 2017

Charge distribution in Neutron Stars

SAKHILE MPILO NDEBELE

Submitted in fulfilment of the academic requirements for the degree of Master of Science School of Mathematics, Statistics and Computer Science College of Agriculture, Engineering and Science

University of KwaZulu-Natal

Durban 2017

As the candidate's supervisor, I have approved this thesis for submission.

Prof Subharthi Ray

Disclaimer

This thesis decribes the work undertaken as a masters degree at the University of KwaZulu Natal. The study in this thesis represents the work of the author and has not been submitted before for any degree to any other institution.

Declaration-Plagiarism

I, Sakhile Mpilo Ndebele, student Number, 207522572 declare that:

1. The research reported in this thesis, except where otherwise indicated, is my original research.

2. This thesis has not been submitted for any degree or examination at any other university.

3. This thesis does not contain other persons' data, pictures, graphs or other information, unless specifically acknowledged as being sourced from other persons.

4. This thesis does not contain other person's writing, unless specifically acknowledged as being sourced from other researchers. Where other written sources have been quoted, then:

a. Their words have been re-written but the general information attributed to them has been referenced

b. Where their exact words have been used, then their writing has been placed in italics and inside quotation marks, and referenced.

5. This thesis does not contain text, graphics or tables copied and pasted from the Internet, unless specifically acknowledged, and the source being detailed in the thesis and in the References sections.

S M Ndebele:

This thesis is dedicated to my late father Mr M.I Ndebele, my late grandmother C.P Ndebele and my Aunt who has just passed on recently A.S Khanyile.

May their soul rest in peace

ACKNOWLEDGEMENTS

I would like to acknowledge everyone who has supported me throughout this study. My special thanks goes to my supervisor Professor Subharthi Ray for his guidance and support from the beginning of this thesis. He has been there for me and very patient with me all the time. He always make sure that I gain the knowledge towards the study of this thesis by his useful feedback on my work . His great assistance and ideas contributed a lot to me towards my ability to produce high quality of work. He played a major role through financial support because I don't think I would have managed without his assistance. Do not be weary in doing good work but continue to be blessing to others. Thank you.

I would also like to thank my mother Mrs T Ndebele who supported me through her prayers and also my sisters Gcwalisile, Ngcebo and Nokuthula. I would like to extend also my sincere appreciation to my uncle N.H Dube he always came to rescue whenever I came across some obstacle and give a solution and a way forward.

Special thanks to my church organisation NATESA they are my home away from home. I have brothers and sisters through NATESA. Finally, I would like to thank all my friends whom I met and shared every moments we had during this study.

Abstract

In previous studies, people have shown that compact stars, like the neutron stars and quark stars, can hold a lot of charge during their formation resulting in a large mass and radius. It was also argued that when the charges leave the system due to repulsion from the self created field, these might render a secondary collapse to a charged black hole. In the present work, we have taken a particular type of charge distribution, with varying parameters, such that changing these parameters mimic the situation when the charge particles leaving the system. We have made a systematic study of each stage of the charge distributions. Our results reveal that when the charge distribution deviates slightly from the scenario where the charge density is proportional to the mass density, then the system is no longer able to retain the large mass and radius, and quickly attains a lower mass and radius.

Contents

Chapter 1

Introduction

Compact stars like neutron stars and quark stars are the stars which are in the final stage of the stellar evolution. A normal star, due to hydrogen burning, radiates out thermal energy. The thermal energy is the one which prevents the collapse of the star due to its own gravitational pull. As the star burns out, and radiates out the heat, then there appears a time when the internal thermal pressure can no longer stand the gravitational pressure and the star collapses. For neutron stars, the ultimate collapse is prevented by the neutron degeneracy pressure and hence they are called neutron stars. Chandrashekhar mass limit shows that a typical neutron star has a mass of 1.4 $M_{\odot}$. It has also been estimated that the radius of a typical neutron star is about 10 km.

One can theoretically obtain the mass radius relation of a neutron star by solving

the Tolman-Oppenheimer-Volkof(TOV) equation, which is the hydrodynamical equilibrium equation. To solve the TOV equations we will need to use the equation of state (EoS), which that shows how the internal pressure is related to the energy density of matter inside the star. Though neutron stars are largely supported by the pressure of degenerate neutrons, the binding of the stars are due to the strong gravitational force in which the matter of the star creates in such a compact regime.

The theoretical concepts of neutron stars dates back to the $1930s$. A dense cloud of neutron gas should support itself from further collapse due to the presence of neutron degeneracy pressure - provided that the total mass is not greater than 2 of Solar Mass ($M_{\odot}$), which is the Chandrashekhar mass limit with the typical neutron star mass to be of $1.4M_{\odot}$. However, the actual prediction for the existence of neutron stars were first done by Baade and Zwicky (1933) - from the observations of the supernova explosions, where they conjectured that in such a process, the centre should collapse to a very dense object of closely packed neutrons, and hence can be a neutron star. Then the other major step was in 1939, when Tolman and independently Oppenheimer and Volkoff developed the hydrostatic equilibrium equation, starting from General relativity - which is useful in the theoretical formulation of the neutron star structure. The idea of neutron stars remained purely a theoretical entity until 1967, when Jocelyn Bell, then a PhD student, observed periodic pulses from a distance radio source which were identified to be neutron

stars emitting pulses of radio waves - radio pulsars. Thus, with the discovery of the radio pulsars, the existence of neutron stars was put on firm ground. Later on, when observation techniques became better and with other wavelengths like the X-rays, it was found that neutron stars were likely to be rotating and can also have intense magnetic fields.

Way back in 1924, Rosseland first pointed out that it might be possibile that normal stars could actually contain a non-vanishing net charge[11]. He modelled the star as a gas of positive ions and electrons and concluded that, due to their greater kinetic energy, the electrons tend to escape from the star more often than normal star. The star will then acquire a net positive charge. The general motion of electrons will then be directed to the top and further escape from the star and will then be stopped by the electric field created by charge separation. Glendening[1] further showed that the maximum electric charge a star can contain should be $Q \sim 100$ Coulomb per solar mass.

The binding of gravity inside a neutron star is many times greater than the nuclei binding that holds atomic nuclei together. Pressure and density vary with depth. Neutron stars are composed primarily of neutrons, protons and electrons. As we go deeper towards the center of the star, the density and pressure increases, and then the strong interactions play an important role near the centre of the star. Some have even conjectured that the centre of a neutron star may not even be a nuclear

matter, but a more compact quark matter. The extreme density range in a neutron star poses a problem to the understanding of the fundamental interactions which are strong interactions and gravity. Hence, neutron stars serves as a melting point for astrophysical studies. One of the underlying problems in studying neutron stars is our limited understanding of the equation of state(EoS) for some nuclear matter.

Now, the introduction of electric charge inside a neutron star makes the situation a bit more complicated. We are now looking at a system, where there are some free protons (carrier of charge, for this charged system). Since the electromagnetic forces are many orders of magnitude larger than the gravitational forces, so, the presence of a few *extra* protons can make the star – now a charged star, highly unstable. In a previous work, Ray *et. al.*[5] have shown that if one assumes the charge distribution of a system varies directly with the matter density, then the system can hold a huge amount of charge - of the order of 10^{20} Coulombs. However, it was also mentioned that lack of any mechanism to bind the electromagnetic force of one proton, to the gravitational force of 10^{18} neutrons, will make the protons to roam around freely inside the star. These protons will also face the strong repulsion from the self created field, and will escape from the star.

The escape of the protons might lead to a secondary collapse of the charged star, and before all the charge leaving the system, this secondary collapse might lead

to the formation of a charged black hole[5]. We borrowed this idea of the charge leaving the system, in our present work, by systematically studying the scenario of five charge distributions that mimic the outflow of the charged particles, starting from the interior and slowly moving out to the surface.

Our work reveals that as soon as we deviate from the particular charge distribution, where the charge density varies directly with the mass density – i.e., when the charge is fractionally pushed out of the centre, and the charge distribution becomes somewhat Gaussian, then the enormous amount of charge the charged star could hold immediately falls down to a very small value. So, the large charge and mass configuration seen in Ray *et. al.*[5], becomes unstable, and quickly attains a lower value. This is also at par with the conjecture of the formation of charged black hole scenario, as mentioned in Ray *et. al.*[5].

In the second chapter of this thesis, we have shown the theoretical formulation of the relevant equations. In the third chapter, we outlined the procedures that we had undertaken for the numerical implementations of the obtained equations. Chapter four gives the results and we make our conclusions in chapter five.

Chapter 2

Mathematical Formulation

The generalisation of the Tolman-Openheimer-Volkof(TOV) equation for a charged star was proposed by Bekenstein[2], who also pointed out many arguments against the stability of the star. For a static, spherically-symmetric system, the metric and the matter content that is described by energy-momentum tensor T can be written in the form

$$ds^2 = e^{\nu}c^2dt^2 - e^{\lambda}dr^2 - r^2(d\theta^2 + \sin^2\theta d\phi^2) \tag{2.1}$$

where ν and λ are the functions of length (r) which represent the gravitational potentials; and

$$T^{\mu}_{\nu} = (P + \epsilon)u^{\mu}u_{\nu} - P\delta^{\mu}_{\nu} + \frac{1}{4\pi}\left(F^{\mu\alpha}F_{\alpha\nu} - \frac{1}{4}\delta^{\mu}_{\nu}F_{\alpha\beta}F^{\alpha\beta}\right) \tag{2.2}$$

respectively,where all the symbols have their usual meanings with the last term in (2.2) coming from the Maxwell's equations. P is the isotropic pressure

and $\epsilon = \rho c^2$ is the energy density of the fluid. The choice of a perfect fluid implies that the flow of matter is adiabatic, there is no heat flow and there is radiation. The fluid four-velocity for the present case can be written as:

$$u_r = u_\theta = u_\phi = 0; \tag{2.3}$$

$$u_0 = e^{-\frac{\nu}{2}};$$

and the electromagnetic field tensor $F^{\mu\nu}$ can be obtained from the four potential A_μ given by

$$F_{\mu\nu} = \frac{\partial A_\nu}{\partial x^\mu} - \frac{\partial A_\mu}{\partial x^\nu} \tag{2.4}$$

satisfying the following equation:

$$\left[\sqrt{-g}F^{\mu\nu}\right]_{,\nu} \;=\; 4\pi j^\mu \sqrt{-g} \tag{2.5}$$

and j^μ is the four-current density.

Since the fluid is static, there are no other contributions to the fluid velocity except the time-like component(μ_0); the velocity is normalized so that $u^t u_t = 1$, where we know that u^μ is the 4-velocity vector. For the time component, one easily sees that $u^t = e^{-\frac{\nu/2}{c}}$ and hence

$$T_{\mu\nu} = \begin{bmatrix} e^{\nu}\epsilon & 0 & 0 & 0 \\ 0 & -e^{\lambda}p & 0 & 0 \\ 0 & 0 & -r^2p & 0 \\ 0 & 0 & 0 & -r^2psin^2\theta \end{bmatrix} \tag{2.6}$$

The Einstein's field equations are given by:

$$R_{\mu\nu} - \frac{1}{2}R\delta_{\mu\nu} = -\frac{8\pi G}{c^4}T_{\mu\nu} \tag{2.7}$$

where,

$$R_{\mu\nu} = \Gamma^{\rho}_{\mu\rho,\nu} - \Gamma^{\rho}_{\mu\nu,\rho} + \Gamma^{\rho}_{\mu\alpha}\Gamma^{\alpha}_{\nu\rho} - \Gamma^{\alpha}_{\mu\nu}\Gamma^{\rho}_{\alpha\rho} \tag{2.8}$$

is the Ricci tensor, and R is the Ricci scalar, found out by contracting the Ricci Tensor.

In the mixed form, we raise the index of both sides of the Einstein's field equation to obtain:

$$R^{\mu}_{\nu} - \frac{1}{2}R\delta^{\mu}_{\nu} = -\frac{8\pi G}{c^4}T^{\mu}_{\nu} \tag{2.9}$$

We now have a simpler form for the energy-momentum tensor T^{μ}_{ν} which we write in matrix from as:

$$T^{\mu}_{\nu} = \begin{bmatrix} \epsilon & 0 & 0 & 0 \\ 0 & p & 0 & 0 \\ 0 & 0 & p & 0 \\ 0 & 0 & 0 & p \end{bmatrix} \tag{2.10}$$

If we solve equation (2.5), we notice that we have non-vanishing term when $\nu = r$ which results to the electric field as:

$$\frac{1}{4\pi}\left(F^{\mu\alpha}F_{\alpha\nu} - \frac{1}{4}\delta^{\mu}_{\nu}F_{\alpha\beta}F^{\alpha\beta}\right) = \frac{-\mathcal{E}^2}{8\pi}$$

where

$$\mathcal{E}(r) = \frac{1}{r^2}\int_0^r 4\pi r^2 j^0 e^{(\nu+\lambda)/2} dr \tag{2.11}$$

is the electric field at a radius r, within the star. If we consider $\mathcal{E}(r) = exp((\nu + \lambda)/2)((d\phi)/dr)$ and if we also consider the charge distribution in some matter as the charge density in proper co-ordinates and denote it as ρ_{ch}, we therefore get the modified equation from (2.11) to be:

$$\mathcal{E}(r) = \frac{1}{r^2}\int_0^r 4\pi r^2 \rho_{\mathrm{ch}} e^{\lambda/2} dr. \tag{2.12}$$

From Einstein's equation, the conditions that when $r = 0$, we have $\mathcal{E}(r) = 0$ and $e^{\lambda/2} = 1$. And at the surface, i.e. for $r = R$, the electric field becomes

$$\mathcal{E}(R) = \frac{Q}{R^2}, \tag{2.13}$$

where

$$Q = \int_0^R 4\pi r^2 \rho_{\rm ch} e^{\lambda/2} dr. \tag{2.14}$$

is the total charge of the system with R as the radius of the star.

Since the present choice of the electromagnetic field is only due to charge, we have only $F^{01} = -F^{10}$ which is non-vanishing, and the other terms are absent.

From Einstein's field equations,

$$e^{-\lambda}\left(\frac{1}{r^2} - \frac{1}{r}\frac{d\lambda}{dr}\right) - \frac{1}{r^2} = -\frac{8\pi G}{c^4}\left(\epsilon + \frac{\mathcal{E}^2}{8\pi}\right) \tag{2.15}$$

$$e^{-\lambda}\left(\frac{1}{r}\frac{d\nu}{dr} + \frac{1}{r^2}\right) - \frac{1}{r^2} = \frac{8\pi G}{c^4}\left(P - \frac{\mathcal{E}^2}{8\pi}\right). \tag{2.16}$$

Using the above two equations, after some manipulations we obtain the following structure equations for the system::

$$\frac{dP}{dr} = -\frac{1}{2}\frac{d\nu}{dr}(P+\epsilon) + \frac{\mathcal{E}}{8\pi}\left(\frac{d\mathcal{E}}{dr} + \frac{2\mathcal{E}}{r}\right) \tag{2.17}$$

$$\frac{d\mathcal{E}}{dr} + \frac{2\mathcal{E}}{r} = 4\pi\rho_{ch} e^{\lambda/2}; \tag{2.18}$$

Equation (2.17) is derived from the vanishing four-divergence of T^{μ}_{ν} and the equation (2.18) is obtained from the general relativistic Maxwell equation.

The charge density in equation (2.18) is our input parameter for our system, along with the equations of state of matter (pressure P vs density ρ). We have chosen the form of the charge density to be somewhat Gaussian, with a slight deviation of the Gaussian peak, for variation of two parameters (a and b). This type of charge density distribution is also a function of the mass density. Varying these two parameters we can see that the Gaussian peak moves from one end to the other in the density variable.

$$\rho_{\rm ch} = \alpha \times \rho \times \left(exp[-(\frac{\rho - a}{b})^2] + 1 \right) \tag{2.19}$$

where, ρ is the mass density, and α is a factor that *tunes* the intensity of the charge density $\rho_{\rm ch}$, so that we can get an acceptable solution. The nature of this variation is shown in figure (3.1). Note that here the stellar surface represent the centre and the stellar centre is represented at the outermost point.

The relation for the integrated mass (at any radius) for the charged system is given by:

$$M(r) = \int_0^r 4\pi r^2 \left(\frac{\epsilon}{c^2} + \frac{\mathcal{E}^2}{8\pi c^2} \right) dr \tag{2.20}$$

and the corresponding metric coefficient is given by:

$$e^{-\lambda} = 1 - \frac{2GM(r)}{c^2 r}. \tag{2.21}$$

This mass $M(r)$, is the total mass as measured from the reference frame of the star itself. However, for a distant observer, which we can refer to as an observer at infinity, the mass is expressed as:

$$\begin{aligned} M_\infty &= \int_0^\infty 4\pi r^2 \left(\frac{\epsilon}{c^2} + \frac{\mathcal{E}^2}{8\pi c^2}\right) dr \\ &= \int_0^R 4\pi r^2 \left(\frac{\epsilon}{c^2} + \frac{\mathcal{E}^2}{8\pi c^2}\right) dr + \int_R^\infty 4\pi r^2 \left(\frac{\epsilon}{c^2} + \frac{\mathcal{E}^2}{8\pi c^2}\right) dr \\ &= M(R) + \frac{Q(R)^2}{2R} \end{aligned} \tag{2.22}$$

where R is the radius of the star. The distant observer will see a contribution of the gravitational potential from the total mass of the charged star, as well as the Coulomb contribution of it.

With this definition of the mass, we can write equation (2.21) in a modified form as:

$$e^{-\lambda} = 1 - \frac{2GM_\infty}{c^2 r} + \frac{GQ^2}{c^4 r^2} \tag{2.23}$$

Now, combining equations (2.15) and (2.16), and the fact that $\lambda(\infty)$ =$\nu(\infty) = 0$, we therefore obtain

$$\nu(r) = -\lambda(r) - e^{\lambda} \quad \int_r^\infty \tfrac{8\pi G r}{c^4} \left(P + \epsilon\right) dr$$

from which we immediately have:

$$\nu(r) = -\lambda(r), \;\; for, \;\; r \geq R \tag{2.24}$$

and

$$\nu(0) = -e^{\lambda} \int_0^{\infty} \frac{8\pi G r}{c^4} \left(P + \epsilon\right) dr \tag{2.25}$$

Using these expressions, the four differential equations λ, ν and μ from the conservation of stress tensor (${T_\nu}^{\mu}{}_{;\mu} = 0$), for the equilibrium of charged stars turn out to be the afore mentioned generalized Tolman-Oppenheimer-Volkoff equation. We can write the hydrostatic equation of equilibrium (equation (2.17)) as

$$\frac{dP}{dr} = -\frac{G\left[M(r) + 4\pi r^3 \left(\frac{P}{c^2} - \frac{\mathcal{E}^2}{8\pi c^2}\right)\right](\epsilon + P)}{c^2 r^2 \left(1 - \frac{2GM(r)}{c^2 r}\right)} + \rho_{\rm ch}\, \mathcal{E}\, e^{\frac{\lambda}{2}}. \tag{2.26}$$

As we can see that the first term on the right hand side comes from the gravitational force with an effective pressure and density. Also coupled within, it is the Coulomb term reducing the effective pressure. Which means the *effective* pressure is *softened* by the presence of the electric charge. The second term on the right hand side comes purely from the Coulomb force, and with a sign opposite to the first term. Irrespective of the nature of the charged particle (the charge comes in square), the presence of this extra coulomb term further reduces the pressure

gradient inside the star. The nett result is that the *effective* equation of state inside the star softens due to the presence of the charge.

Chapter 3

Numerical Implementation

3.1 The numerical integration procedure

The modified TOV equation is a coupled differential equation, with the pressure term appearing both in the differential form on the left hand side, and on the right hand side along with the rest of the terms. To solve such equations, there can be several ways - both analytically and numerically. We have taken the numerical approach. We have used a FORTRAN program to compute the solution numerically.

3.1.1 The 4-point Runge Kutta method

Within the FORTRAN program, our equations were solved using the 4-point Runge-Kutta method. The basic outline for this method is described as below:

Let an initial value problem be specified as follows:

$$\dot{y} = f(t, y), \quad y(t_0) = y_0.$$

Let y be an unknown function (scalar or vector) of a variable t, which we would like to approximate; we are told that $\dot{y}$, the rate at which y changes, is a function of t and of y itself. At the initial time t_0 the corresponding y value is y_0.

The function f and the data t_0, y_0 are given.

Now pick a step-size $h > 0$ and define

$$y_{n+1} = y_n + \tfrac{h}{6}\left(k_1 + 2k_2 + 2k_3 + k_4\right),$$

$$t_{n+1} = t_n + h$$

for $n = 0, 1, 2, 3, ...$, using:

$$k_1 = f(t_n, y_n),$$
$$k_2 = f\left(t_n + \frac{h}{2}, y_n + h\frac{k_1}{2}\right),$$
$$k_3 = f\left(t_n + \frac{h}{2}, y_n + h\frac{k_2}{2}\right),$$
$$k_4 = f\left(t_n + h, y_n + hk_3\right).$$

Here y_{n+1} is the RK4 approximation of $y(t_{n+1})$, and the next value (y_{n+1}) is determined by the present value (y_n) plus the weighted average of four increments, where each increment is the product of the size of the interval, h, and an estimated slope specified by function f on the right-hand side of the differential equation.

$\rightarrow$ k_1 is the increment based on the slope at the beginning of the interval, using y (Euler's method);

$\rightarrow$ k_2 is the increment based on the slope at the midpoint of the interval, using $y + \frac{k_1}{2}$;

$\rightarrow$ k_3 is again the increment based on the slope at the midpoint, but now using $y + \frac{k_2}{2}$;

$\rightarrow$ k_4 is the increment based on the slope at the end of the interval, using $y + k_3$.

3.1.2 The Interpolation

The FORTRAN code also reads the EoS from a separate external file, where there are gradually increasing 40 points that are generated from a polytropic function, and covering the entire range. However, these 40 discrete points are insufficient to perform the integration in the Runge-Kutta method, and hence we also had to deploy an interpolation technique. Because the range of values are large, we used a logarithmic interpolation technique.

Let (P_j, ρ_j) and (P_{j+1}, ρ_{j+1}) be two successive points in the EoS table. In order to obtain any the intermediate value (P, ρ), the logarithmic interpolation should be:

$$\frac{\log P - \log P_j}{\log \rho - \log \rho_j} = \frac{\log P_{j+1} - \log P_j}{\log \rho_{j+1} - \log \rho_j} \tag{3.1}$$

The integration of the TOV starts at the centre of the star. At each stage, each of these interpolated values (P, ρ) are called inside the Runge-Kutta subroutine, for an increase in the radius of the star. The centre of the star has a maximum density, and as it integrates out, the density decreases, and so also the pressure. The integration stops at a point where the pressure P becomes zero, which is by definition, the equilibrium between the interior and the exterior – the surface of the star.

3.2 Modification to the equations

In order to make the equations consistent with the Runge Kutta approach, we have to make all the integration equations to a differential form. So, we have the following sets of differential equations:

(a) The modified TOV equation:

$$\frac{dP}{dr} = -\frac{G\left[M(r) + 4\pi r^3\left(\frac{P}{c^2} - \frac{\mathcal{E}^2}{8\pi c^2}\right)\right](\epsilon + P)}{c^2 r^2\left(1 - \frac{2GM(r)}{c^2 r}\right)} + \rho_{\rm ch}\,\mathcal{E}\,e^{\frac{\lambda}{2}}. \tag{3.2}$$

(b) The differential form for the electric field:

$$d\mathcal{E} = -\frac{2\mathcal{E}dr}{r} + 4\pi\rho_{\rm ch}e^{\lambda/2}dr, \tag{3.3}$$

(c) The differential form for the mass:

$$dM = 4\pi r^2\left(\frac{\epsilon}{c^2} + \frac{\mathcal{E}^2}{8\pi c^2}\right)dr \tag{3.4}$$

(d) The differential form for the metric coefficient λ can be deduced from the two equations (2.15) and (2.16), so that we have

$$d\lambda = \left[\frac{8\pi G}{c^2}re^{\lambda}\left(\frac{\epsilon}{c^2} + \frac{\mathcal{E}^2}{8\pi c^2}\right) - \left(\frac{e^{\lambda} - 1}{r}\right)\right]dr. \tag{3.5}$$

So, we now have a set of 4 differential equations, which can be solved simultaneously within our FORTRAN code, with an input of the EoS data.

Note that there are four unknown functions and the boundary conditions for the solution are, at the centre where $r = 0$, the electric field $\mathcal{E}(r) = 0$, the metric

coefficient $e^{\lambda(r)} = 1$, the central pressure $P(r) = P_c$, and the central density $\rho(r) = \rho_c$, are the maximum; and at the surface where $r = R$, the pressure $P(r) = 0$. The inputs in the equations are the pressure P, the energy density ϵ and the charge density ρ_{ch}. The metric coefficient λ and the electric field $\mathcal{E}$ are interdependent. This gives us a set of four coupled differential equations (3.2, 3.3, 3.4 and 3.5), which we solve simultaneously to get our results. We also note that since the electric field appears in the mass term (3.4) and the pressure gradient term (2.26) in squares, and also in the Coulomb part, the product $\rho_{\text{ch}}\mathcal{E}$ is invariant, so the form of these equations are not affected by the sign of the charge - i.e. to say that the charge particles can be either electrons or protons.

3.3 The Input parameters

3.3.1 The polytropic equation of state

We considered the case of a self-gravitating completely degenerate fermion system which is much simpler than considering any model-dependent equation of state. A very general approach is to consider a polytropic equation of state of matter. As the EoS of matter is a relation between the density of the matter (ρ) and its pressure (P), we can relate the two in the polytropic form as:

$$P = \kappa\rho^{1+1/n} \tag{3.6}$$

where κ is a normalization constant and n is the polytropic index which is related to the exponent Γ as $n = \frac{1}{\Gamma-1}$. The benefit of using such a form of the EoS is that, varying the polytropic index one can attain the equation of state of matter both in the relativistic regime and in the non-relativistic regime. The other benefit is to have a simpler form for the relation between the pressure and the density, which otherwise is very complicated for a system like the neutron star, with lots of nuclear process and interactions happening between the particles inside the matter. Now, in the relativistic regime, the *allowed* value of Γ is 1.33 to 1.66. If we consider the case of $\Gamma = \frac{5}{3}$ (=1.66), then the corresponding value of n is 1.5. In our numerical code we have primarily used the units and dimensions for the pressure and density in units of (MeV/fm^3). So, to match with the dimensions, we had to choose a value of κ as 0.05 $[fm]^{8/3}$.

3.3.2 The charge distribution

The charge density $(\rho_{\rm ch})$ is chosen to be of the Gaussian type, mapped on the matter density, such that with the variation of matter density (ρ), the charge density too will follow a similar pattern but with a Gaussian bump, mimicking the situation that the charged particles are pushed outwards due to the self created fields. So, to attain such a form we have assumed the following form of the charge dis-

tribution.

$$\rho_{\rm ch} = \alpha \times \rho \times \left\{ exp \left[- \left(\frac{\rho - a}{b} \right)^2 \right] + 1 \right\} \tag{3.7}$$

The parameters a and b changes the position and width of the Gaussian peaks, ρ is the mass density, and α is a parameter that *tunes* the charge content, so that we can determine what is the right fraction of this function (i.e., the right fraction of the charge distribution) that can be allowed to give a stable and consistent result.

For our charge density ρ_{ch}, we have taken 5 sets of values for the parameters a and b, and called them *Distribution1, Distribution2,* ..., etc, and then worked out the maximum mass for each of these distributions for different charge fractions α. In Table (3.1), we have shown the different values of the parameters that we chose for the different charge distributions. With all these inputs, we execute

Table 3.1: Variation of parameters for charge distribution.

$Distributions$	a	b
1	3.9	0.9
2	2,8	1.1
3	1.9	0.9
4	1.2	0.7
5	0.5	0.2

our FORTRAN code to obtain the desired results. We plot the outputs using the

GNUPLOT software package.

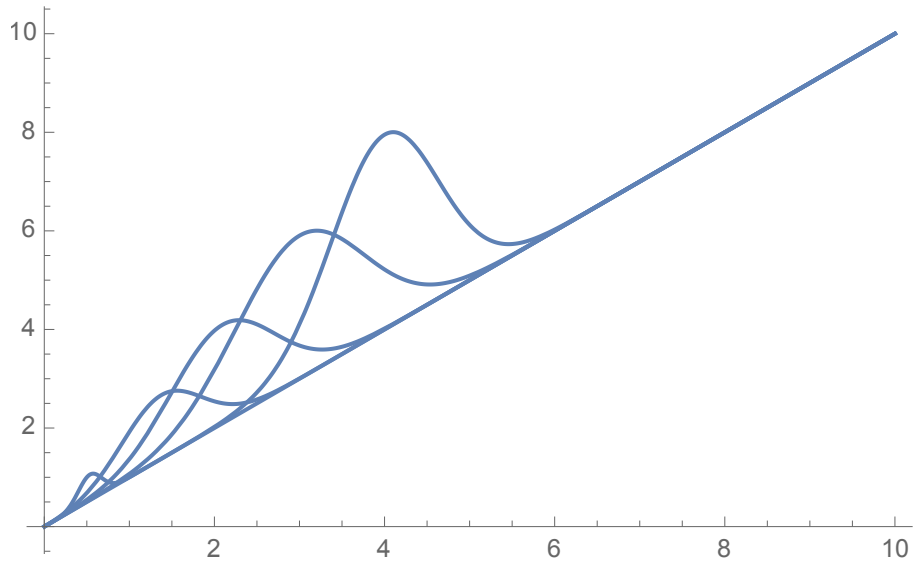

Figure 3.1: Variation of the charge density (ρ_{ch}) (y-axis) vs the matter density (ρ) (x-axis). Since the central density is maximum, and the surface density is zero, for a polytropic neutron star, so the nature of the charge densities also follow accordingly. The rightmost peak is for Distribution1 and the leftmost peak is for Distribution5.

Chapter 4

Results

In Table (4.1), we show the maximum mass for different charge fractions and their corresponding radii for five different charge distributions that we have.

In Figures (4.1)-(4.5) we show the mass-radius relation for all the five charge distributions for different values of the charge fraction α. A careful inspection reveals us that although the maximum mass star for all the five charge distributions are in the range 1.6-1.8 $M_{\odot}$, yet, the charge distribution 1 (with the Gaussian peak of the charge density closer to the centre) has a slightly higher value for the maximum mass than the others, and the trend follows for the other charge distributions too.

In Figures (4.6)-(4.10), we have shown the variation of charge density (from centre to the surface) inside the maximum mass star,

Table 4.1: The maximum allowed Mass-Radius for different distributions with corresponding maximum values of charge fraction α it could reach.

Distributions	M_{tot} ($M_\odot$))	R (km)	Corresponding value of α
1	1.959	13.282	0.000475
2	1.624	13.448	0.0003
3	1.589	13.546	0.000285
4	1.587	13.673	0.0003
5	1.715	13.448	0.00045

for different values of charge fraction. The nature of the curves clearly indicates the nature of charge distribution we have assumed, with a slight variation due to the gravitational effects. The units are in geometric units.

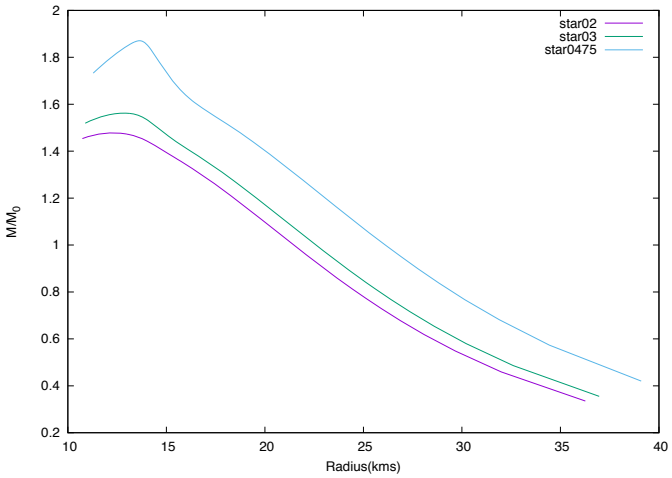

Figure 4.1: Mass-Radius relation for different values of α, for charge distribution 1.

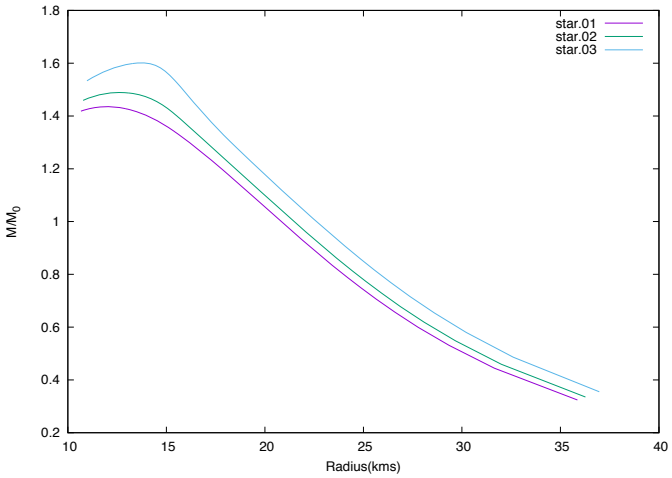

Figure 4.2: Mass-Radius relation for different values of α, for charge distribution 2.

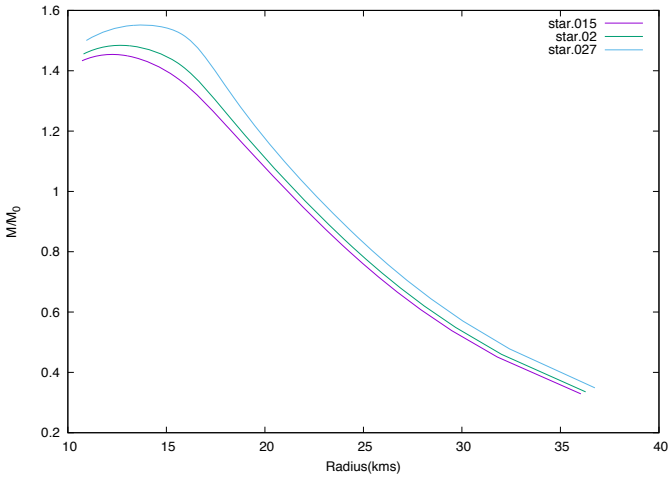

Figure 4.3: Mass-Radius relation for different values of α, for charge distribution3.

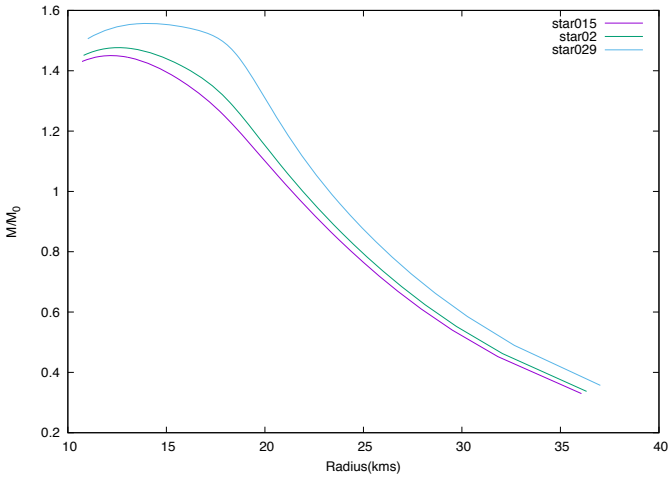

Figure 4.4: Mass-Radius relation for different values of α, for charge distribution4.

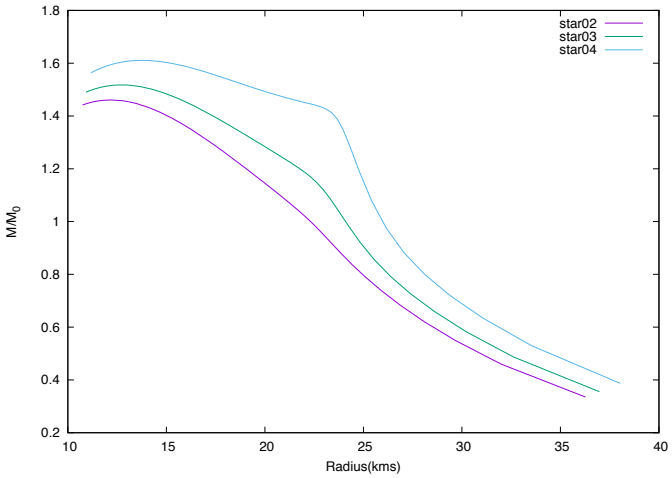

Figure 4.5: Mass-Radius relation for different values of α, for charge distribution5.

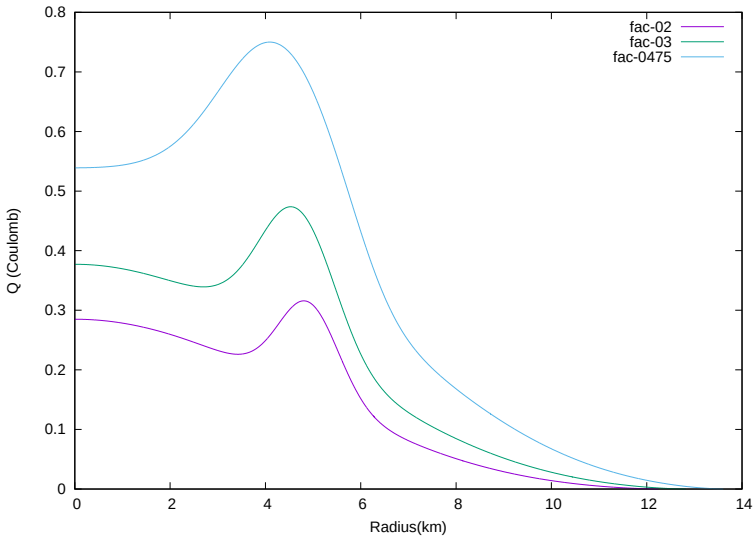

Figure 4.6: The variation of the charge density with radius for different α, for charge distribution1.

In Figure (4.11), we plotted the metric coefficient e^{λ} as a function of radius for the maximum mass star for each of the charge fractions, for all five different distributions. If we look at the nature of e^{λ} is the same for all the stars with different charges. We found that there is a slight change for higher charge fractions thus showing the gain in the compactness $(\frac{M}{R})$ of the star with charge.

In Figure (4.12), we have shown the variation of the charge with the radius for the maximum mass star (and maximum charge they can hold) for each of the 5 charge distributions. The units are again in geometric units.

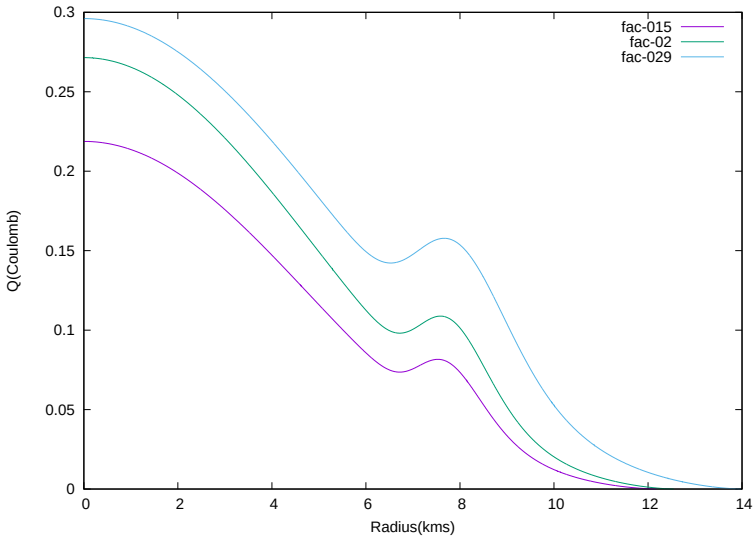

Figure 4.7: The variation of the charge density with radius for different α, for charge distribution2.

The next analysis was done to check the nature of the pressure gradients $\frac{dp}{dr}$ for all the five charge distributions. From Figures (4.13)-(4.17), we see that the nature is more or less remain the same with larger intensity of charge (i.e., larger values of α) making the pressure gradient softer. It is also noteworthy that for distribution 1, the $\frac{dp}{dr}$ plot for higher values of α flattens out more, showing that for charges concentrated more towards the centre, the TOV equation tends to allow larger maximum mass star.

Finally, we have analysed the metric coefficient (e^{λ}) for the maximum mass stars,

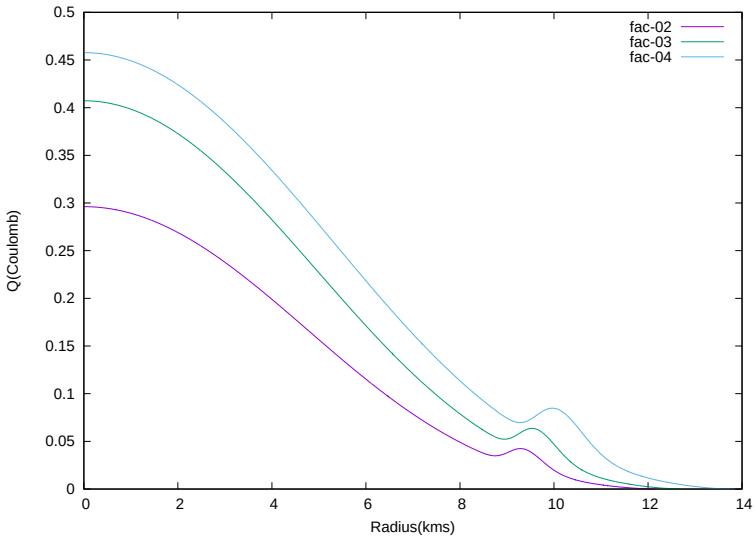

Figure 4.8: The variation of the charge density with radius for different α, for charge distribution3.

for each for different values of α, for all the five distribution types. They are shown in Figures (4.18)-(4.22). For higher charge fraction, the peak of the curves shift to the right. For Figure (4.18), the height of the peaks are different from the rest of the four types of distributions, which could be because of the presence of higher charge near the centre of the star.

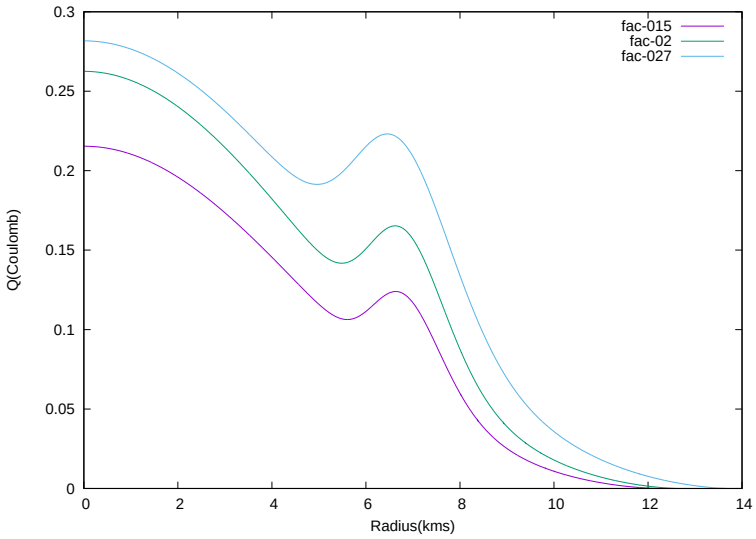

Figure 4.9: The variation of the charge density with radius for different α, for charge distribution4.

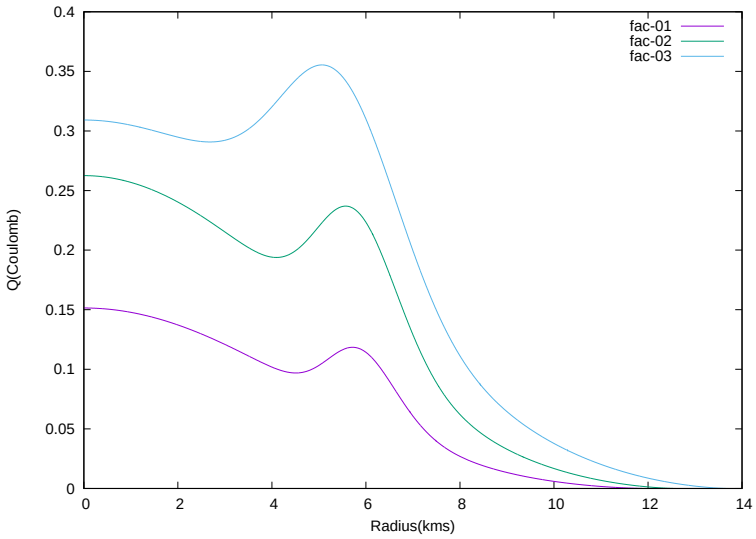

Figure 4.10: The variation of the charge density with radius for different α, for charge distribution5.

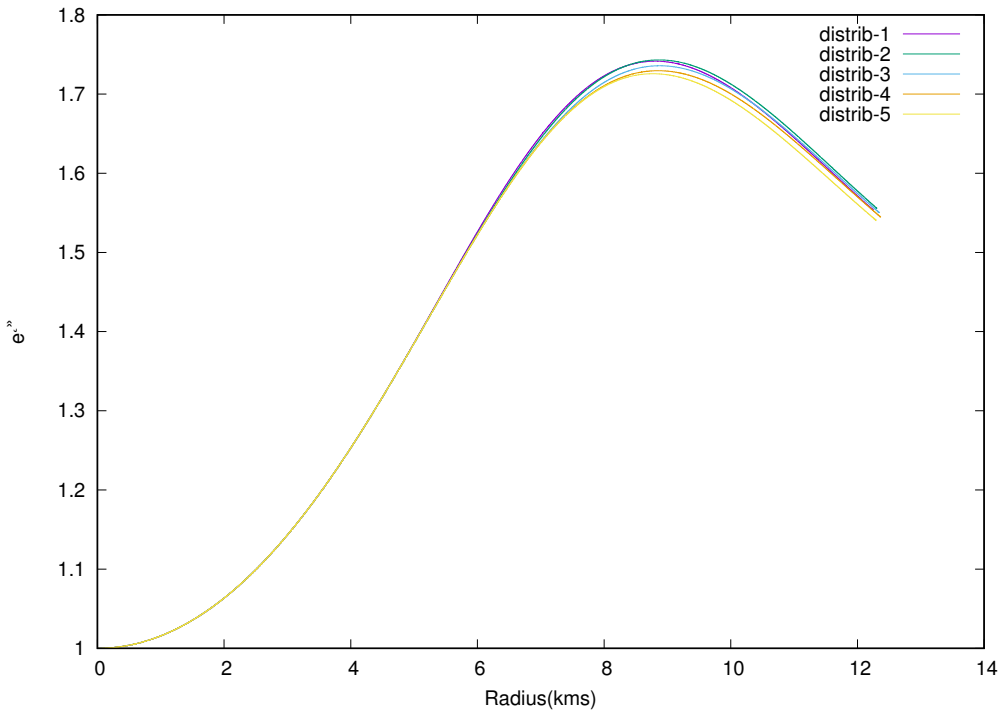

Figure 4.11: The variation of the metric e^{λ} with the radius in the maximum mass stars for different cases of charge distribution

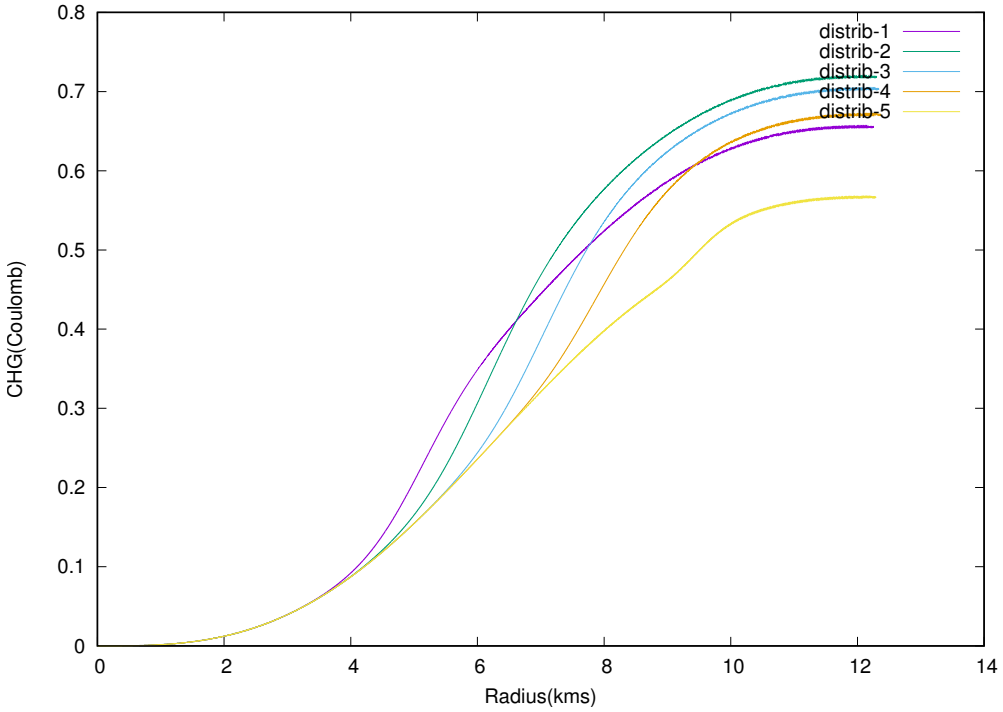

Figure 4.12: Total charge with radius of the star in maximum mass

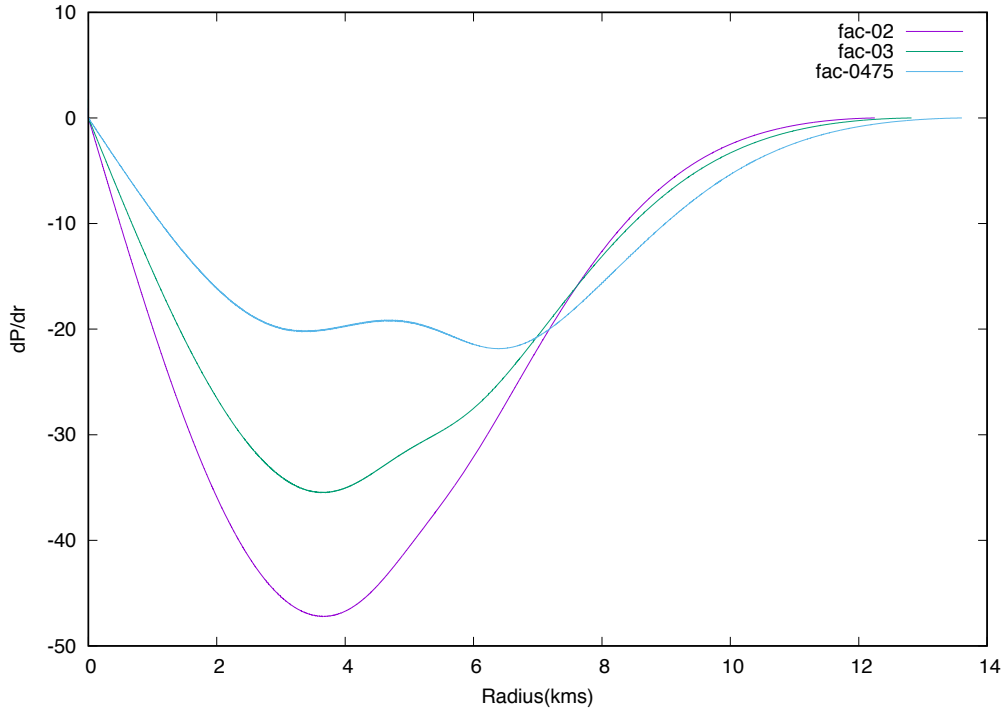

Figure 4.13: dp/dr for distribution 1, for different values of the charge fraction α.

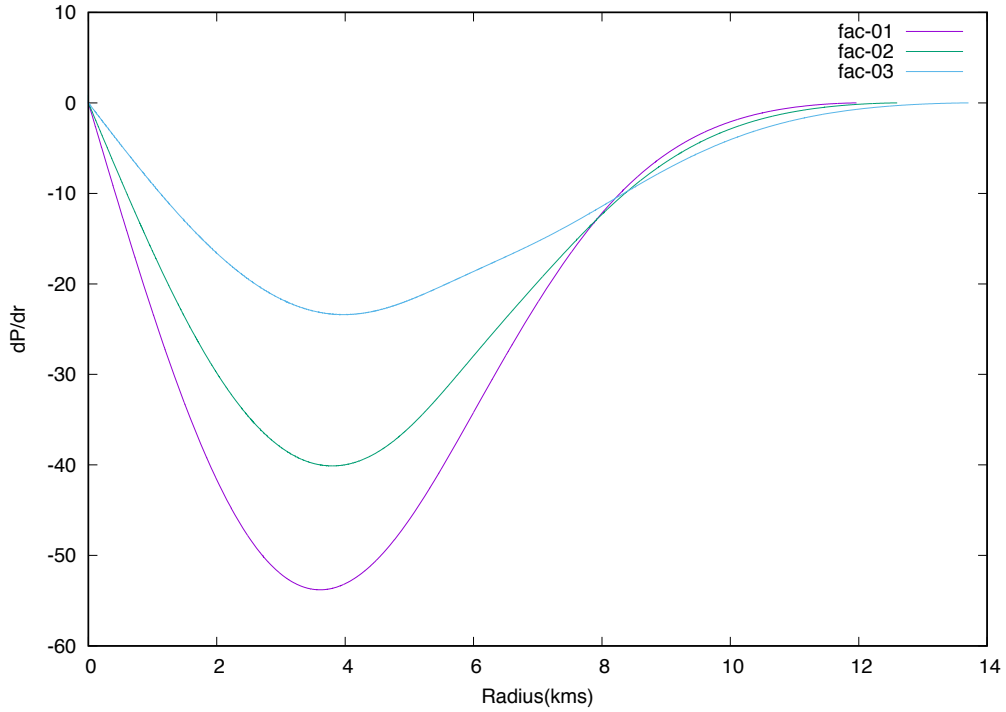

Figure 4.14: dp/dr for distribution 2, for different values of the charge fraction α.

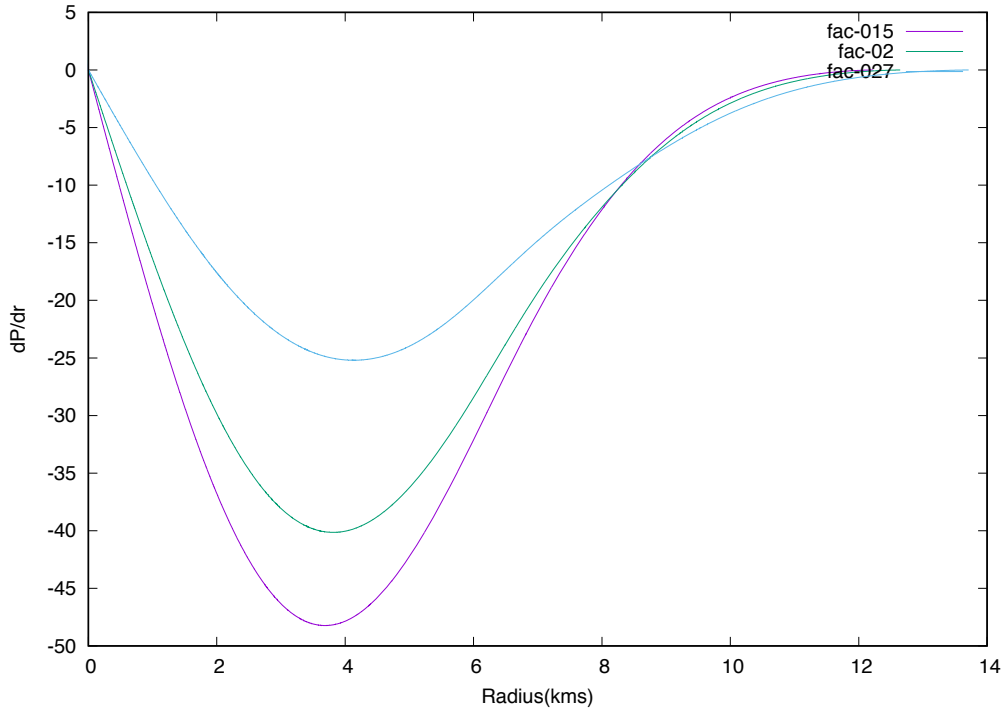

Figure 4.15: dp/dr for distribution 3, for different values of the charge fraction α.

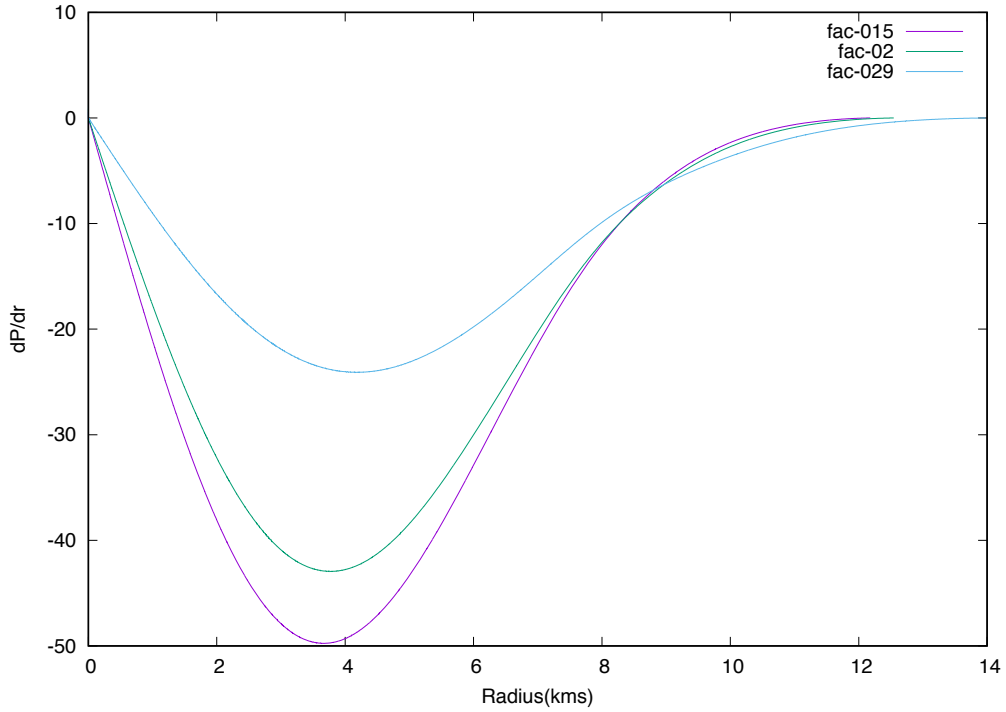

Figure 4.16: dp/dr for distribution 4, for different values of the charge fraction α.

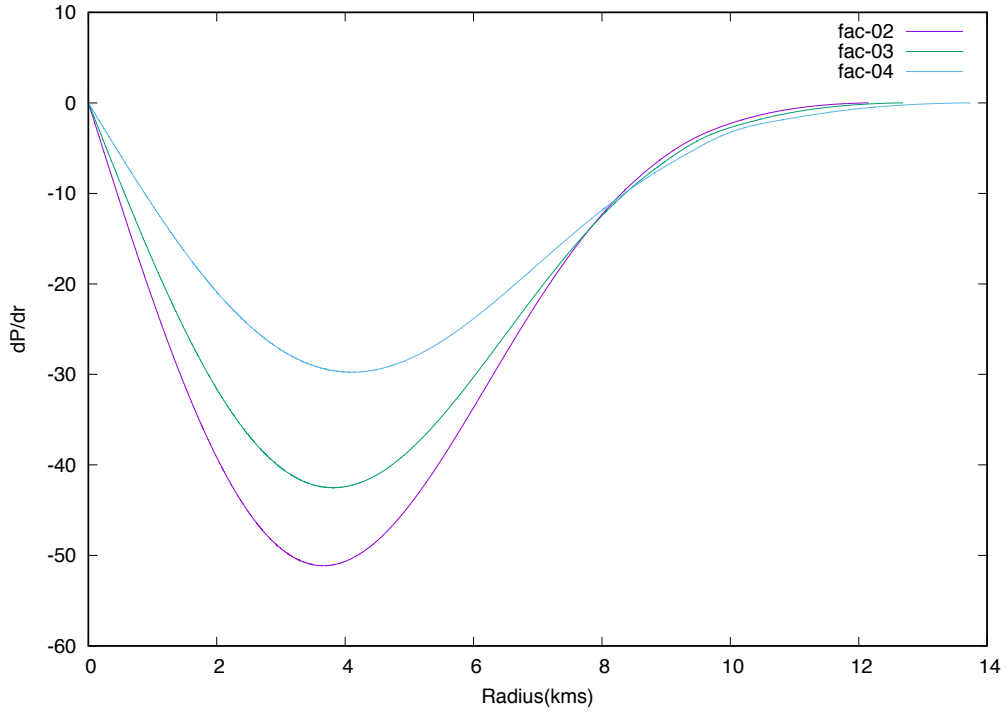

Figure 4.17: dp/dr for distribution 5, for different values of the charge fraction α.

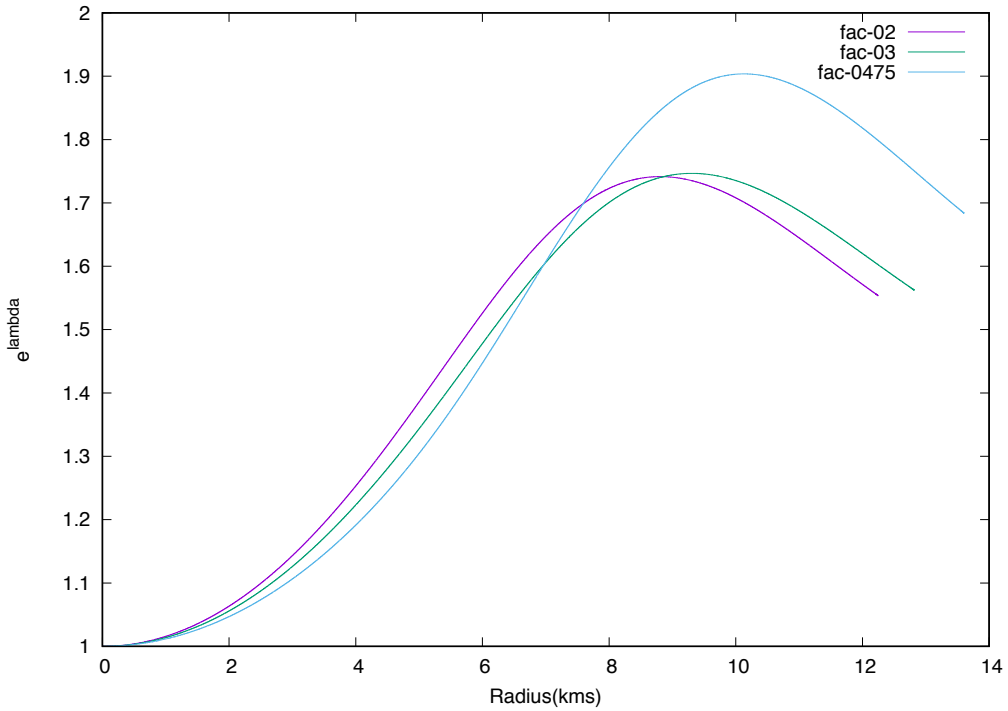

Figure 4.18: The metric coefficient e^{λ} against the radius for the maximum mass star for distribution 1, for different values of the charge fraction α.

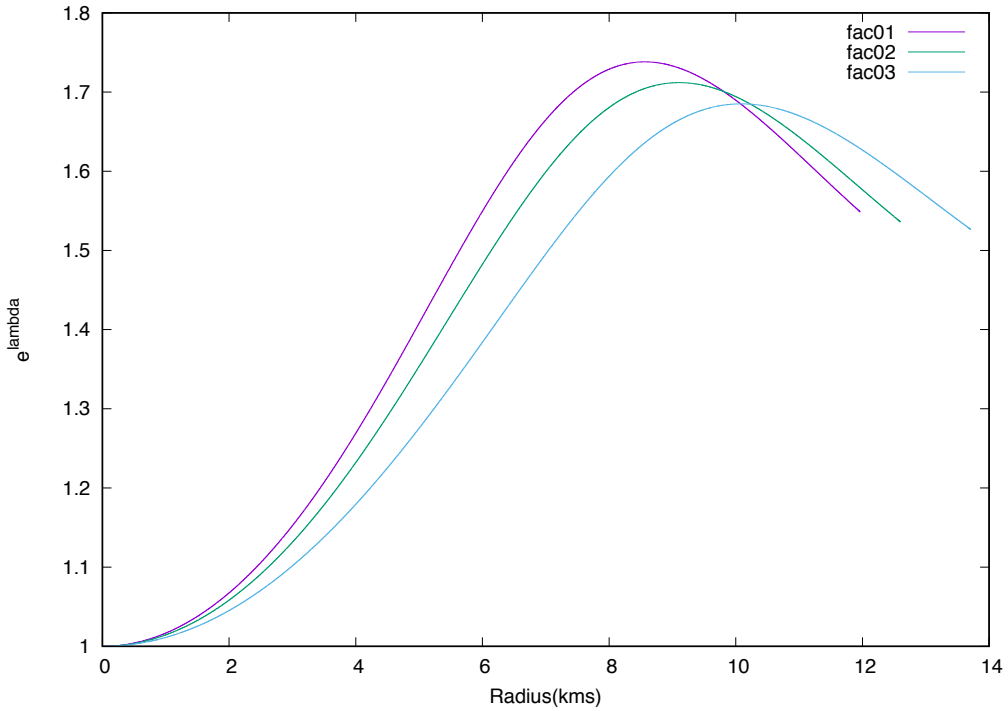

Figure 4.19: The metric coefficient e^{λ} against the radius for the maximum mass star for distribution 2, for different values of the charge fraction α.

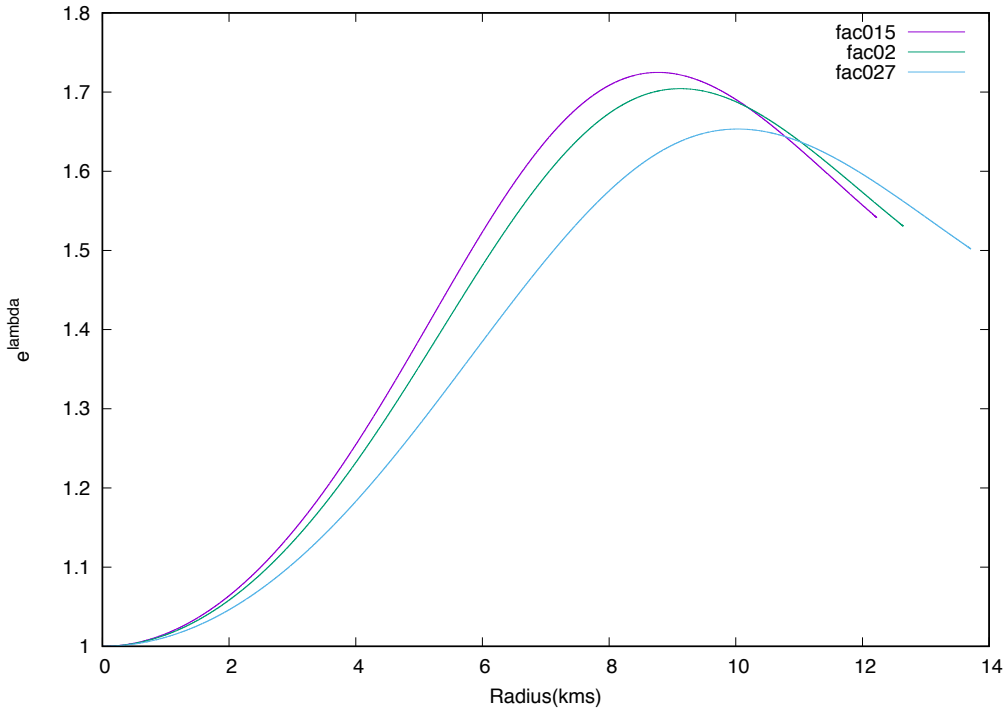

Figure 4.20: The metric coefficient e^{λ} against the radius for the maximum mass star for distribution 3, for different values of the charge fraction α.

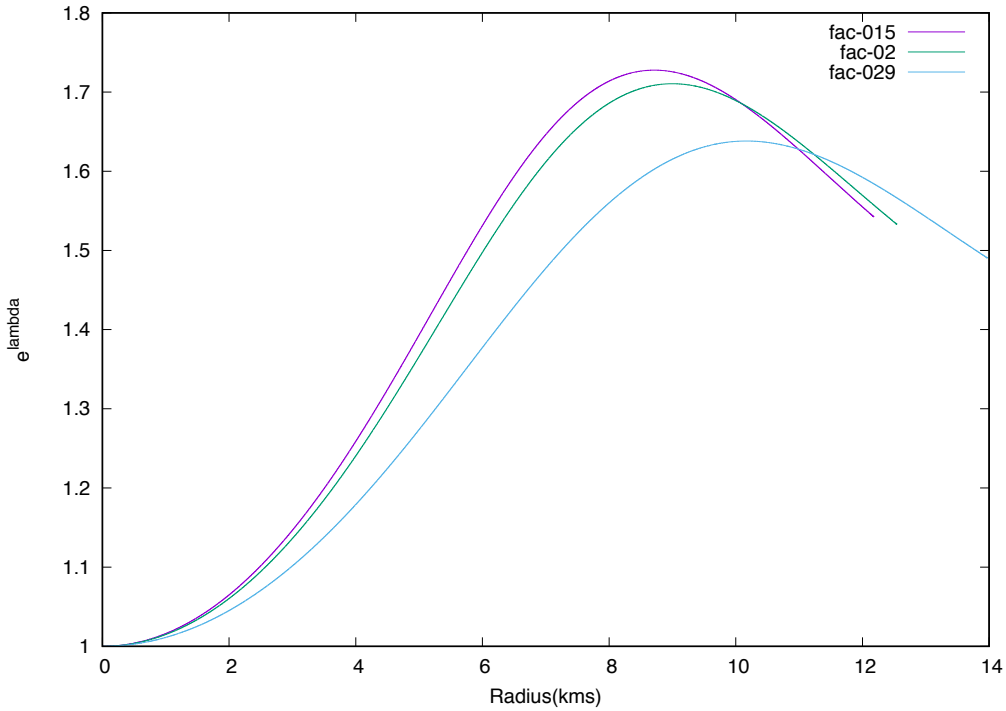

Figure 4.21: The metric coefficient e^{λ} against the radius for the maximum mass star for distribution 4, for different values of the charge fraction α.

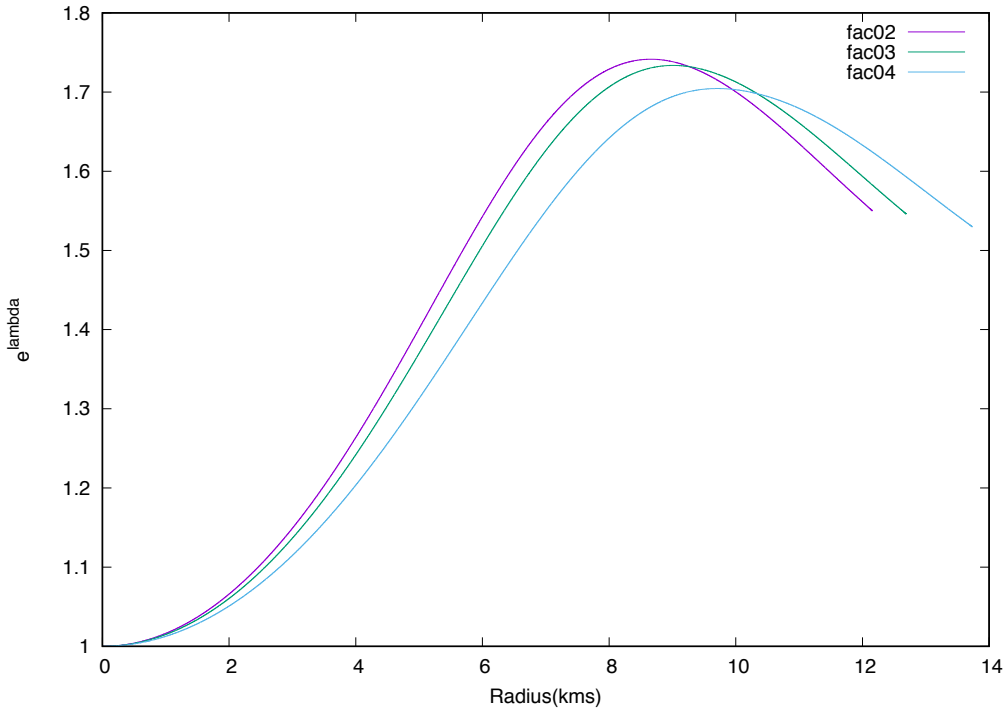

Figure 4.22: The metric coefficient e^{λ} against the radius for the maximum mass star for distribution 5, for different values of the charge fraction α.

Chapter 5

Discussion and Conclusion

Generally speaking, the amount of charge that can be contained in neutron star can be very high and are many orders of magnitude larger than those calculated by classical balance of forces at the surface of a star. Ray *et al.*[5] showed that the charge can be as high as 10^{20} Coulomb to bring in any change in the mass-radius relation of the star, yet remaining stable as long as one considers only the hydrostatic equilibrium and the global balance of forces. The primary concern for such a highly charged star was from the containment of the charged particles with the neutral particles. For a neutron star to hold $\sim 1\ 10^{20}$ Coulomb of charge, the electromagnetic force of 1 extra proton balances the gravitational force of 10^{18} chargeless neutrons. So, for the bulk system, that is seemingly okay. However, if one looks at the free extra proton, then there is no reason why it will remain

constrained with this set of neutrons, and hence there will be a motion on the free protons.

The self created electric field for these free *extra* protons will be huge, and will act on each of these free protons, from the centre of the spherical star. Hence the proton will be free to move outwards inside the star. Presence of other protons and neutrons and other sub-atomic particles will add some physical resistance to the free motion, and hence the motion of the free protons will be something like a *random walk with a direction*. A complete study for this leakage of charge from a highly charged neutron star, requires an intensive numerical simulation. For this project what we considered is to take, say, 5 instances of the charge leakage process, and worked out the detailed morphologies of the charged stars during these instances.

Before we infer on our results, we must like to point out that the central density plays a very important role in determining the maximum mass that can be formed from an equation of state of matter. For the charged star case, the central mass-energy density, is enhanced by similar amount coming from the electrostatic energy density (vide equation (2.20)). Adding to the cause, the modified TOV equation (vide equation (2.26)) also gets *softened* due to the presence of the charge terms – which means that the integration process continues further for larger values of the radius, and hence a larger mass and charge of the charged star.

These has been shown in Ray *et al.,*[5].

Turning back to our situation, we notice that we are unable to obtain larger values for the mass and radius of the charged system, when the central value of the charge density is substantially lower than the mass density. This is the scenario when the charged particles have been pushed outwards by the self created field. The central (energy) density then primarily remained as that of only from the contribution from the mass density. This nature has been depicted from the mass-radius curves for all the five types of charge distributions that we have studied. If we compare the maximum allowed charge for all the five charge distributions, we find that the variation between one from the other is very little, and is far away from the maximum attained mass of $\sim 4.3\ M_{\odot}$. The similarity of the nature for the metric function for maximum mass of the five distributions, as shown Figure (4.11), also affirms our inference.

One may argue that the pressure gradient (dp/dr of the TOV equation) is softened by the presence of the charge density, and should allow for larger maximum mass star. Our inference here is that, yes, it does change the value for the maximum mass, but not substantially, because the central density (and hence the central pressure) for the star receives almost negligible contribution from the electrostatic energy due to the presence of the charged particles.

So, we can conclude that if the charge density at the core of the charged polytropic

neutron star reduces due to the expulsion of the charged particles by the self created field, then the maximum mass drops down to nearly its non-charged configuration. This reaffirms the claim made in Ray *et al.,*[5] that as the charged particles leave the system, there might be a secondary collapse resulting in the formation of a charged black hole. We also conclude that the higher mass-radius configuration attained for a charged polytropic neutron star, is because of the choice of the charge density, where it varied linearly with the mass density. Any deviation from it, and in particular, if the central density does not have a substantial contribution from the charge density, then the formation of higher mass and extremely high charged system might not be possible.

Bibliography

[1] N. K. Glendenning, *Compact Stars: Nuclear Physics, Particle Physics, and General Relativity*, Springer-Verlag (2000).

[2] J. D. Bekenstein, Phys. Rev. D **4** (1971) 2185.

[3] J. L. Zhang, W. Y. Chau and T. Y. Deng, Astrophys. and Space Sc. **88** (1982) 81.

[4] F. de Felice, Y. Yu and Z. Fang, Mon. Not. R. Astron. Soc. **277** (1995) L17.

[5] S. Ray, A. L. Espindola, M. Malheiro, J. P. S. Lemos and V. T. Zanchin, Phys. Rev. D **68** (2003) 084004.

[6] F. de Felice, S. M. Liu and Y. Q. Yu, Class. Quantum Grav. **16** (1999) 2669.

[7] Y. Q. Yu and S. M. Liu, Comm. Teor. Phys. **33** (2000) 571.

[8] P. Anninos and T. Rothman, Phys. Rev. D **65** (2001) 024003.

[9] S. D. Majumdar, Phys. Rev. D **72** (1947) 390.

[10] M. K. Mak, P. N. Dobson Jr. and T. Harko, Europhys. Lett. **55** (2001) 310.

[11] S. Rosseland, Mont. Not. Royal Astronomical Society **84** (1924) 720.

[12] A. R. Taurines, C. A. Z. Vasconcellos, M. Malheiro and M. Chiapparini, Phys. Rev. C **63** (2001) 065801.

[13] N. K. Glendenning, F. Weber and S. A. Moszkowski, Phys. Rev. C **45** (1992) 844.

[14] A. S. Eddington, Internal Constitution of the stars, Cambridge University Press, Cambridge, England, 1926.

[15] J. Bally and E. R. Harrison, ApJ **220** (1978) 743.

[16] B. B. Siffert,J.R.T. de Mello Neto, and M. O. Calvao , Phys. Rev. D Vol.37 no. 2B (2007) 37.

[17] Christian G. Bohmer,General Relativity, Univeristy College London , Phys. Rev. D (2008) .